Nuclear Engineering and Technology 54 (2022) 2579–2585

Contents lists available at ScienceDirect

Nuclear Engineering and Technology

journal homepage: www.elsevier.com/locate/net

Original Article

Towards effective indirect radioisotope energy converters with bright and radiation hard scintillators of $(Gd,Y)_3Al_2Ga_3O_{12}$ family

M. Korzhik [a, b, *], R. Abashev [c], A. Fedorov [a, b], G. Dosovitskiy [b, d], E. Gordienko [b, d], I. Kamenskikh [e], D. Kazlou [a], D. Kuznecova [b, d], V. Mechinsky [a, b], V. Pustovarov [c], V. Retivov [b, d], A. Vasil'ev [f]

[a] Institute for Nuclear Problems of Belarus State University, Minsk, Belarus
[b] National Research Center "Kurchatov Institute", Moscow, Russia
[c] Ural Federal University, Yekaterinburg, Russia
[d] NRC "Kurchatov Institute" – IREA, Moscow, Russia
[e] Physical Department of Moscow State University, Moscow, Russia
[f] Skobelchin Institute for Nuclear Physiocs of Moscow State University, Moscow, Russia

ARTICLE INFO

Article history:
Received 31 October 2021
Received in revised form
16 December 2021
Accepted 7 February 2022
Available online 15 February 2022

Keywords:
Indirect converter
Beta-voltaics
Alpha-voltaics
Quaternary garnet
Terbium
Cerium
Radiation hardness

ABSTRACT

Ceramics of quaternary garnets $(Gd,Y)_3Al_2Ga_3O_{12}$ doped with Ce, Tb have been fabricated and evaluated as prospective materials for indirect energy converters of α-and β-voltaic. Samples were characterized at excitation with an X-ray source and an intense 150 keV electron beam and showed good temperature stability of their emission and tolerance to irradiation. The role of X-rays accompanied the α-particle emitting in the increase of the conversion efficiency is clarified. The garnet-type structure of the matrix in the developed materials allows the production of quality crystalline mass with a light yield exceeding that of the commonly used YAG: Ce scintillator by a factor of two times.

1. Introduction

Long life radioisotope-based direct-conversion nuclear batteries created by coupling of radioactive sources to a semiconductor element were found to be prospective for use as long-living power supplies of different purposes [1–3]. The sources of highly ionizing charged particles emitted by radioisotopes are of particular interest due to a high energy density deposition in the solid state [4]. At the high flux of the ionizing particles from isotope source a radiation damage of the converter occurs. A utilization of wide-band or liquid semiconductors partly resolves this problem [5,6]. Moreover, as higher band gap of semiconductor is, as better conversion efficiency is achievable [7]. Recently, a few types of direct-conversion devises have been reported [8–11] including evaluation of α-voltaic unit based on diamond coupled to ^{241}Am source [12].

Indirect conversion of ionizing radiation, which uses an intermediate conversion of the ionizing radiation in the optical photons with further their absorption in a photovoltaic element (PV), eliminates the problem of the radiation damage of the conversion material. This creates an opportunity to use cheap silicon photo-sensors, the shock of radiation damage will be taken by the luminescent intermediate converter, which blocks the penetration of charged particles into the PV element. Naturally, cathodoluminescence phosphors have been considered for this purpose first [13–17]. However, bright phosphors of ZnS and $(Y,La,Gd)_2O_2S$ families are produced in a polycrystalline form, even thin layers of which demonstrate a sufficient light scattering, which deteriorates light collection from the converters made of them. A possible solution is to use renewable liquid scintillator [18] however, it complicates the design, and liquid scintillators have a low stopping power to ionizing radiation and a limited light yield by nature.

* Corresponding author. Institute for Nuclear Problems of Belarus State University, Minsk, Belarus.
E-mail address: mikhail.korjik@cern.ch (M. Korzhik).

https://doi.org/10.1016/j.net.2022.02.007

Inorganic crystalline scintillators might be the pool of materials to choose as prospective intermediate converters. Various branches of nuclear science and technology, including safety at nuclear power plants, high-energy physics, security applications, nuclear medicine [19], drove the development of scintillators last few decades. In particular, involving high-luminosity particle emitters, like proton colliders [20] demanded the development of radiation hard scintillation materials for detecting the ionizing radiation. A systematic study of the radiation effects in inorganic oxide crystalline scintillation materials [21–30] resulted in the development of several families of irradiation-tolerant Ce doped materials: aluminates and gallates with garnet structure and oxyorthosilicates. Comparison of several scintillation materials for intermediate converters purpose is in Table 1. A layer of the scintillator with thickness less than 100 μm would be enough to settle a radiation damage of PV. Oxide scintillation materials mechanically robust and non-hygroscopic. Halides, $LaBr_3$ and $GdBr_3$, have high light yield however, possess an affinity to water and must be encapsulated to operate in the Earth's environment. Oxyorthosilicates, namely Lu_2SiO_5:Ce and $(Lu,Y)_2SiO_5$:Ce have high light yield under γ-quanta excitation however, demonstrate as twice as high γ/α ration (~10) in a comparison with garnets. It limits their application for alpha-voltaics. This put forward the application of garnet-type materials for indirect-conversion nuclear batteries. Garnet structure has cubic crystalline symmetry; single crystals of a large diameter may be obtained by Czhochralski or micro-pulling-down methods [31]. In addition, garnets can be produced as transparent ceramics by hot pressing or, in a translucent form by 3D printing [32,33].

Recently, we demonstrated that the light yield of Ce- and Tb-doped scintillators can be drastically improved by substituting ternary by quaternary garnets as the matrix material [34,35]. Quaternary Gd-based garnets are of a particular interest. At their high concentration in the matrix, Gd ions form a sublattice resulting in sub-bands inside the band gap, the lowest of which is built by $^6P(^7f)$ state. Sub-bands play twofold role: prevent creation of the stable colour centres in the crystal under irradiation and, form a reservoir for Frenkel-type excitons (FTE) having typically energy close to the energies of transitions $^8S \rightarrow {}^6P$(~3.9eV). Therefore, the density of FTE in the crystal is, at the same energy deposited, larger in a comparison with the lattice excitons having energies near the bottom of the conduction band. This increases the scintillator efficiency to the level of the most efficient sulphide phosphors [36].

Moreover, a variation of the composition of cations in Gd-based matrices allows fine-tuning of the resonance conditions between FTE and the Rare Earth (RE) ions introduced into the matrix acting as emission centres. This capability encouraged us to engineer scintillators based on quaternary garnets with a general formula $(Gd,Y,RE)_3Al_2Ga_3O_{12}$ (RE = Tb, Ce) suitable to provide the highest light yield under electron beam excitation. The data on light yield obtained under high flux beam made possible an evaluation of the efficiency of the conversion both under α- and β-particles of different isotope sources. We focused on the development of the scintillators in a ceramic form. In comparison with a single crystal of the corresponding composition, ceramics is less expensive to produce and enable substantially higher doping levels of the garnet matrix, which is of especial importance to avoid activator saturation at intense excitation.

2. Materials and methods

Coprecipitation method was used to produce fine powders with various compositions and doping of $(Gd,Y,RE)_3Al_2Ga_3O_{12}$ (RE = Tb, Ce). It exploits mixing all the desired components in a solution and provides a homogeneous product allowing phase formation at lower temperature, which is favourable to suppresses Ga evaporation. Mixed nitrate solutions containing Gd, Y, Ce, Tb, Al, and Ga in appropriate ratios to produce materials corresponding to formulas listed in Table 1, were prepared from Gd, Y, Tb oxides (purity of 4N5, 5 N, and 4 N, respectively), aluminum hydroxide (5 N) and gallium and cerium nitrates (4N5 and 3N5) had the concentration of 1 mol/L. Then, the mixed solution was slowly added to 2 mol/L solution of NH_4HCO_3 under constant stirring to form a precipitate. The precipitate was filtered, washed with water twice and with isopropyl alcohol once, dried at 100 °C in air ventilated oven for 8 h and calcined at 850 °C for 2 h. Afterward, the powder was milled down to a median particle size of 1.0–1.5 μm in a planetary ball mill in corundum grinding media.

Ceramic samples were prepared from the powders to test with beam and X-ray excitation:1.5 mm-thick green bodies of 20 mm in diameter were prepared by uniaxial pressing at 64 MPa. The tablets were sintered in air at 1600 °C for 2 h. The resulting ceramics samples had the density of ~98% of the theoretical value, had certain porosity, but were noticeably translucent. A SEM image of a typical ceramics sample (Jeol JSM 7100 F), mirror-polished and thermally etched at 1250 °C, is presented in Fig. 1(a). The samples were ground to a thickness of 1 mm for study of their emission properties. The luminosity of the Tb doped sample under electron beam is in Fig. 1(b).

The list of the samples studied is given in Table 2. The concentration of Ce in the samples was approximately by a factor of ten higher than the typical concentration of Ce (~1000 ppm) used in single-crystalline Al–Ga garnets pulled from the melt. Such a relatively high Ce concentration was chosen to diminish the phosphorescence intensity in the crystalline samples, which is typical for Ga–Al mixed crystals without additional codoping by aliovalent ions as used for the mixed single crystals production [37]. The concentration of Tb was chosen to be close to the value providing the highest luminescence yield in Al-based garnets, as it is reported in Ref. [38]. Another important issue which can be resolved with a high concentration of activation ions is a preventing of the ground state depletion at high excitation intensity [39]. It is shown that Tb doped $Y_3Al_3O_{12}$ have better tolerance to saturation in a comparison with widely used sulphide Zn(Cd)S(Ag) [40]. Prior to the measurements with X-ray and electron beam sources, the light yield of the samples having fast scintillation kinetics was evaluated with moderate sources of α-particles and γ-quanta

Table 1
Some properties of oxide crystalline scintillation materials doped with Ce.

Material	Density, g/cm^3	Attenuation of α-particles 5 MeV (99,9%), μm	Attenuation of β-particles 150 keV (99,9%), μm	LY, γ-excitation, ph/MeV	Reference, radiation tolerance confirmed at irradiationwith γ-quanta or proton fluence above 10^{14}p/cm^2
Lu_2SiO_5	7.48	14.5	35.5	27000	[23]
$Y_3Al_5O_{12}$	4.55	17.3	65.5	30000	[26]
$Gd_3Al_2Ga_3O_{12}$	6.68	16	43.5	43000	[29]
$(Gd,Y)_3Al_2Ga_3O_{12}$	5.86	16.7	50	52000	[34]

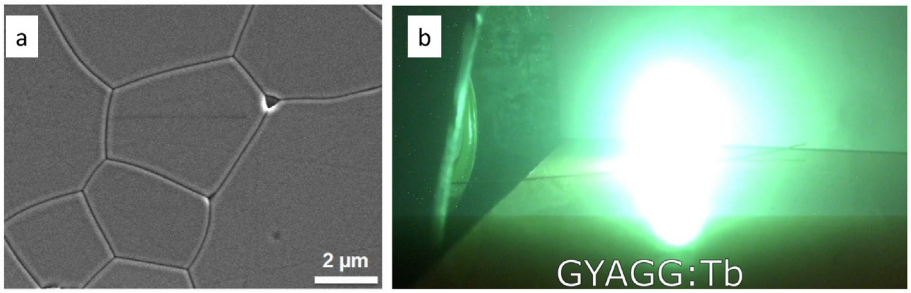

Fig. 1. Scanning electron microscopy image of $Gd_{1.13}Y_{1.72}Tb_{0.15}Al_2Ga_3O_{12}$ sample (**a**), this sample under excitation with 150 keV electron beam, current density 1A/cm^2 (**b**).

Table 2
Compositions of GYAGG scintillators studied and light yields (LY) obtained at different excitations.

Sample	Composition	LY, γ-excitation, ph/MeV	LY, α-excitation, ph/MeV	γ/α
1	$Gd_xY_{2.85-x}Tb_{0.15}Al_2Ga_3O_{12}$(x = 0.53) (GYGAG1)	104500	48850[a]	[d]
2	$Gd_xY_{2.85-x}Tb_{0.15}Al_2Ga_3O_{12}$(x = 0.83) (GYGAG2)	159600	74600[a]	[d]
3	$Gd_xY_{2.85-x}Tb_{0.15}Al_2Ga_3O_{12}$(x = 1.13) (GYGAG3)	147400	68850[a]	[d]
4	$Gd_xY_{2.85-x}Tb_{0.15}Al_2Ga_3O_{12}$(x = 1.43) (GYGAG4)	135600	65350[a]	[d]
5	$Gd_xY_{2.85-x}Tb_{0.15}Al_2Ga_3O_{12}$(x = 0.59) (GYGAG5)	105000	49000[a]	[d]
6	$Gd_xY_{2.85-x}Tb_{0.15}Al_2Ga_3O_{12}$(x = 2.03) (GYGAG6)	79000	36900[a]	[d]
7	$Gd_xY_{2.97-x}Ce_{0.03}Al_2Ga_3O_{12}$(x = 1.19) (GYGAG7)	42500[b]	15200	2.8
8	$Gd_xY_{2.97-x}Ce_{0.03}Al_2Ga_3O_{12}$(x = 1.19) (GYGAG8)	36000[b]	12800	2.8
9	$Y_{2.97}$ $Ce_{0.03}Al_5O_{12}$:Ce (YAG1)	25000[b]	4200	5.9
10	$Y_{2.97}Ce_{0.03}Al_5O_{12}$:Ce (YAG2)	23000[b]	3800	6
11	$Gd_{2.85}Tb_{0.15}Al_2Ga_3O_{12}$(GAGG)	33800	15800	2.14[c]

[a] LY measured under α-particles excitation in a current mode of PMT [35] with ^{241}Am source (10^4Bq).
[b] LY of the samples having fast scintillation kinetics and measured under ^{137}Cs(10^4Bq) 662 keV γ-quanta excitation.
[c] The γ/α ratio was measured under α-particles excitation of ^{241}Am and γ-quanta of ^{137}Cs sources at shaping time 77.5μs.
[d] The γ/α ratio was chosen as measured with single crystal GAGG:Tb (Sample #11).

(662 keV) in pulse height mode. A single crystal sample $Gd_{2.85}Tb_{0.15}Al_2Ga_3O_{12}$(GAGG) was used for measurement of γ/α ratio. Surface of the crystal was grinded to mimic ceramic samples. Pulse height spectra were measured with Photomultiplier Hamamatsu R329 at a shaping time constant of 77.5μs. This shaping time was ~30 times less than scintillation decay time in GAGG; however, it was enough to acquire pulse-height spectra with prominent photo-and full-absorption peaks from γ-quanta and α-particles. The ratio was measured to be 2.14 ± 0.2 or, ~30% less than 2.8, which was measured for Ce doped GYAGG ceramics samples and applied to evaluate the LY of Tb doped samples in [35]. Ceramics and single crystal Tb doped samples were assessed for light yield under α-particles in a current mode described elsewhere [35]. These data and the LY calculated results for γ-quanta utilising measured γ/α ratio are listed in Table 1 as well.

The luminescence properties of the fabricated samples were evaluated under excitation by X-rays and electron beam. The X-ray excited luminescence (XRL) spectra were measured at excitation by apparatus URS-55A equipped with X-ray tube BSV-2 (Cu anode, 30 kV, 10 mA). The luminescence was dispersed using LOMO monochromator MDR-23 and detected by photomultiplier FEU-106 in a photon-counting mode. The spectral resolution was 2 nm. A small-size pulsed accelerator MIRA-2D with electron tube IMA-2-150E (electron energy 150 keV, current density 1 A/cm^2, pulse duration ~ 20 ns) was used for excitation in the cathodoluminescence (CL) spectroscopy experiments. It corresponds to the 1 cm^2 surface activity provided by certain amount of the 100% enriched β-isotope as follows: ^{63}Ni-0.12g;^{147}Pm-0.0073g; ^{14}C-1.51g. Therefore, measurements have been performed in the irradiation conditions close to the conditions of the further exploiting. The CL spectra were recorded using Oriel Instruments spectrograph FICS 77443 (uncooled CCD detector, spectral resolution 2.4 nm, ~0.34 nm/pixel) by collecting the luminescence at ~45° to the direction of electron beam. To avoid signal saturation in the detection system with a limited dynamic range, a 0.18 mm-thick Al filter was installed at the output of the electron tube. The absorbed dose

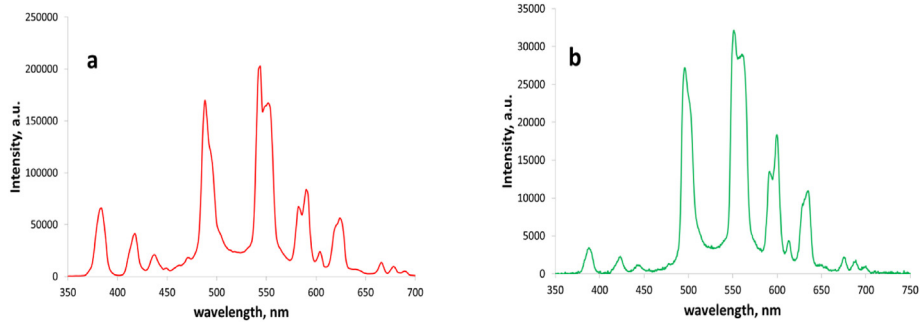

Fig. 2. XRL (a) and CL(b) room temperature spectra of sample GYAGG2.

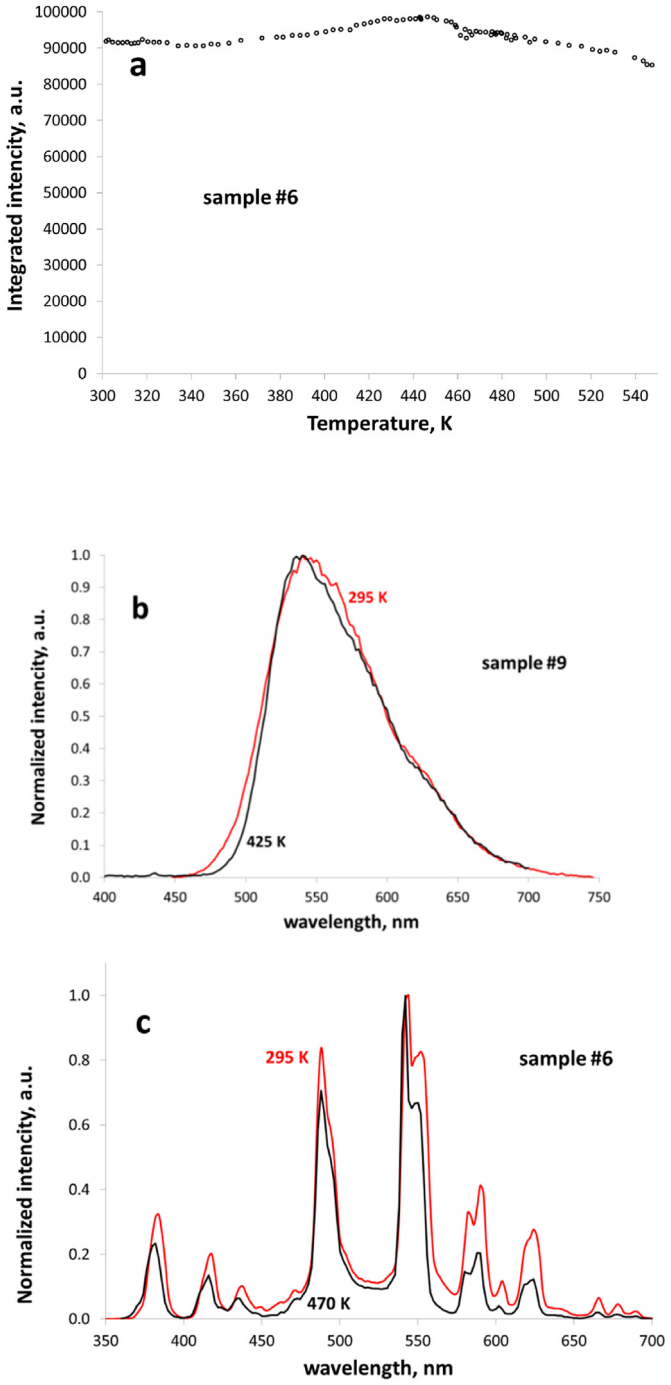

Fig. 3. XRL yield temperature dependence of the GYGAG6 sample (**a**) and comparison of spectral reproducibility measured at 295 and 425 K for YAG1 and 295 and 470 K for GYAGG6 correspondingly (b,c).

during the exposure was measured by using certified film dosimeter SO PD (E) −1/10 "VNIIFTRI" and measuring the induced optical density at a wavelength of 550 nm. At an absorbed dose rate of 0.5 kGy/s, the absorbed dose was 2.0 kGy. We also applied higher dose rates of both ionizing radiation sources to estimate the sample performance at intense irradiation and to reveal their possible degradation.

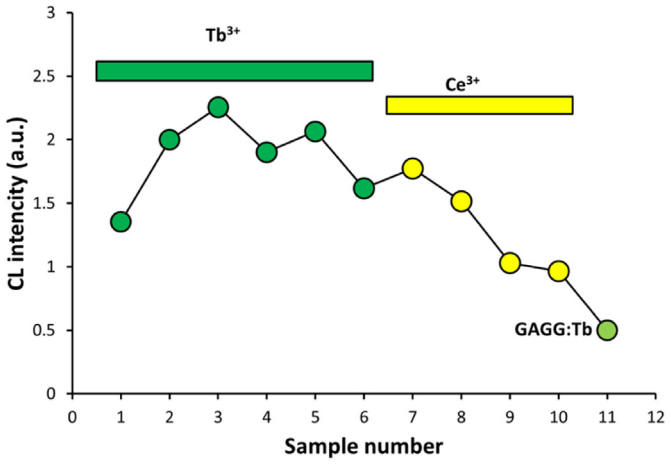

Fig. 4. CL intensity integrated in the spectral range 300–800 nm for the samples listed in Table 1. The dopants are indicated by horizontal bars, the intensity is normalized to that of YAG:Ce.

3. Results

The comparison of luminescence spectra of $Gd_xY_{2.85-x}Tb_{0.15}Al_2Ga_3O_{12}$ (x = 0.83) under X-ray and electron beam excitations are presented in Fig. 2. In general, the scintillation spectra are typical of Tb^{3+} ions in quaternary Gd–Y garnet-type crystals [35] and the emission lines are distributed over the entire visible range. The blue part of the spectrum is caused by transitions $^5D_3 \rightarrow {}^7F_j$, whereas the luminescence bands in the range 475–725 nm are caused by transitions $^5D_4 \rightarrow {}^7F_j$. A decrease in the intensity of the transitions in the blue part of the spectrum is observed. This might be explained by increasing the role of intracenter nonradiative relaxation from $^5D_3$ to $^5D_4$ at the condition of depletion of the ^7F_j ground state.

The stability of the luminescence spectrum and weak efficiency degradation of the material with increasing temperature are crucially important parameters for nuclear battery applications with a high-energy deposition at excitation. Fig. 3 demonstrates XRL spectra integrated intensity versus temperature of GYAGG6 sample and its spectral reproducibility in temperature range. Similarly, to Ce-doped YAG garnet, GYAGG doped with Tb shows the spectral stability over the visible range.

Worth noting, Tb-doped sample shows a small temperature coefficient for the light yield LY(T) in the temperature range 300–540 K. YAG:Ce under such conditions of excitation demonstrates LY(T) −0.22%/°C, respectively. GYAGG:Ce demonstrates the stability of the luminescence intensity distribution as well, however, its LY(T) is by a factor of three larger than that in YAG.

The comparison of the cathodoluminescence LY of the samples with that in YAG:Ce, which can be considered as a reference sample, is shown in Fig. 4. Tb doped samples show the highest LY and the similar trend for LY change versus Gd/Y ratio as described in Ref. [35]. All samples are superior to YAG:Ce (samples #9 and #10), which is an extensively used garnet-based phosphor. As seen, GAGG:Tb scintillator demonstrates only 50% of YAG:Ce light yield.

4. Discussion

An evaluation of the materials light yield at high flux excitation is a crucial point for further estimation of the module power provided. We assume that Ce doped materials are not saturated due to

Table 3
Estimated energy conversion efficiency in indirect-conversion nuclear batteries having two scintillator plates coupled to the layer of the radioisotope on a base of developed scintillation materials.

Isotope	Scintillation material	LY, ph/MeV	Scintillator conversion efficiency	[a]Radiosotope specific power, mW/cm^2	Nuclear battery specific power, mW/cm^2	Nuclear battery energy efficiency
^{63}Ni,	GYAGG2 (Tb)	55200	0,215	0,695	0,142	0,204
0.12 g/cm^2	GYAGG7(Ce)	42500	0,166	0,695	0,109	0,158
^{147}Pm	GYAGG2 (Tb)	55200	0,215	2,485	0,508	0,204
0.0073 g/cm^2	GYAGG7(Ce)	42500	0,166	2,485	0,391	0,158
^{238}Pu	GYAGG2 (Tb)	25800	0,10	17,04	0,830	0,193
(0.03 g/cm^2)	GYAGG7(Ce)	15200	0,059	17,04	0,480	0,196
^{241}Am	GYAGG2 (Tb)	25800	0,10	2,24	0,106	0,096
(0.02 g/cm^2)	GYAGG7(Ce)	15200	0,059	2,24	0,063	0,112

[a] Estimated following to [3].

Table 4
An additional specific power of provided by soft X-rays from^{238}Pu and^{241}Am sources on 0.1 mm thick GYAGG scintillator.

Isotope	Soft X-rays, keV	Intensity rel. to alpha decay, %	Spec. power in 0.1 mm thick GYAGG from gamma, mW/cm^2	Total spec. power in 0.1 mm thick GYAGG from gamma, mW/cm^2
^{238}Pu	11,62	0,25	1,06E-04	0.075
(0.03 g/cm^2	13,6	4,2	2,92E-02	
	15,4	0,102	1,63E-05	
	17,06	5,2	4,39E-02	
	20,3	1,15	1,93E-03	
	43,5	0.0395	5,63E-07	
	99,85	0,00735	5,00E-09	
^{241}Am (0.02 g/cm^2)	11,87	37	3,05E-01	0.360
	26,3446	2,27	7,08E-04	
	32,183	0,0174	2,86E-08	
	33,196	0,126	1,40E-06	
	42,704	0,0055	1,50E-09	
	43,42	0,073	2,54E-07	
	55,56	0,0181	1,65E-08	
	59,5409	35,9	5,51E-02	
	98,97	0,0203	5,13E-09	
	102,98	0,0195	4,30E-09	

the fast scintillation kinetics avoiding Ce^{3+} ground state depletion. Therefore, γ/α ratio remains the same as shown in Table 2. A comparison of the integrated intensities in Fig. 4 shows that the highest LY of the Tb based samples (#2) is 55200 ph/MeV. The fact that yield of scintillation in Tb doped sample under intense electron beam drops down suggests that the luminosity under α-particles will show similar behavior. It can be elucidated if we take into account that Tb scintillation kinetics constant is 2 ms and, therefore, depletion of the ground state can lead to a drop in the scintillation yield. Finally, assuming that γ/α is kept we conclude that LY under the intense flux of α-particles should be at least 25800 ph/MeV. As seen, both Ce and Tb doped materials are fitted well for both types of exciting particles.

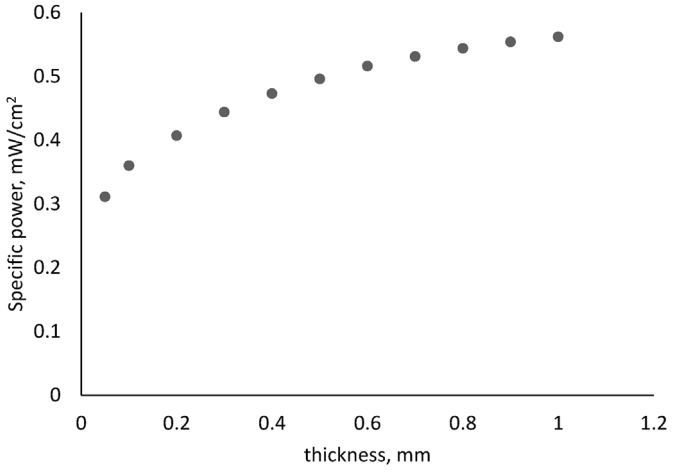

Fig. 5. Specific power deposited into the scintillator of different thickness by soft X-rays of ^{241}Am.

The results of estimation of the efficiency of the beta- and alpha-voltaics having two scintillator 1 cm^2 plates coupled to the 1 cm^2 layer of isotope in between them with weight indicated in the first column are in Table 3. In the estimation of nuclear battery efficiency, we have neglected self-absorption of α- and β-particles, set the light collection coefficient to 0.95, the PV cell energy efficiency to 0.5 [41] and doubled the result due to two-sided PV design. Scintillation conversion efficiency for β-particles is rather consistent with the results obtained for soft γ-quanta [42].

As seen, overall conversion efficiency can reach up to 10% at the use of developed materials. At the operation, some drop of the conversion efficiency is expected at the heating however, this effect is less pronounced in Tb doped scintillator as seen from Fig. 3(a). Worth noting, both Pu and Am sources emit soft X-rays. Table 4 summarizes specific power from soft X-rays accompanied emitting of α-particles by ^{238}Pu and ^{241}Am. A sufficient contribution of X-rays absorption in the specific power deposited in scintillator is recognized in a case of ^{241}Am source. Fig. 5 shows change of specific power deposited into the scintillator by soft X-rays on its thickness.

So, use of the 0.5–0.6 mm thick scintillator plate play twofold role: resolving the problem of the radioprotection and gain in the specific power deposited at the level of 20%.

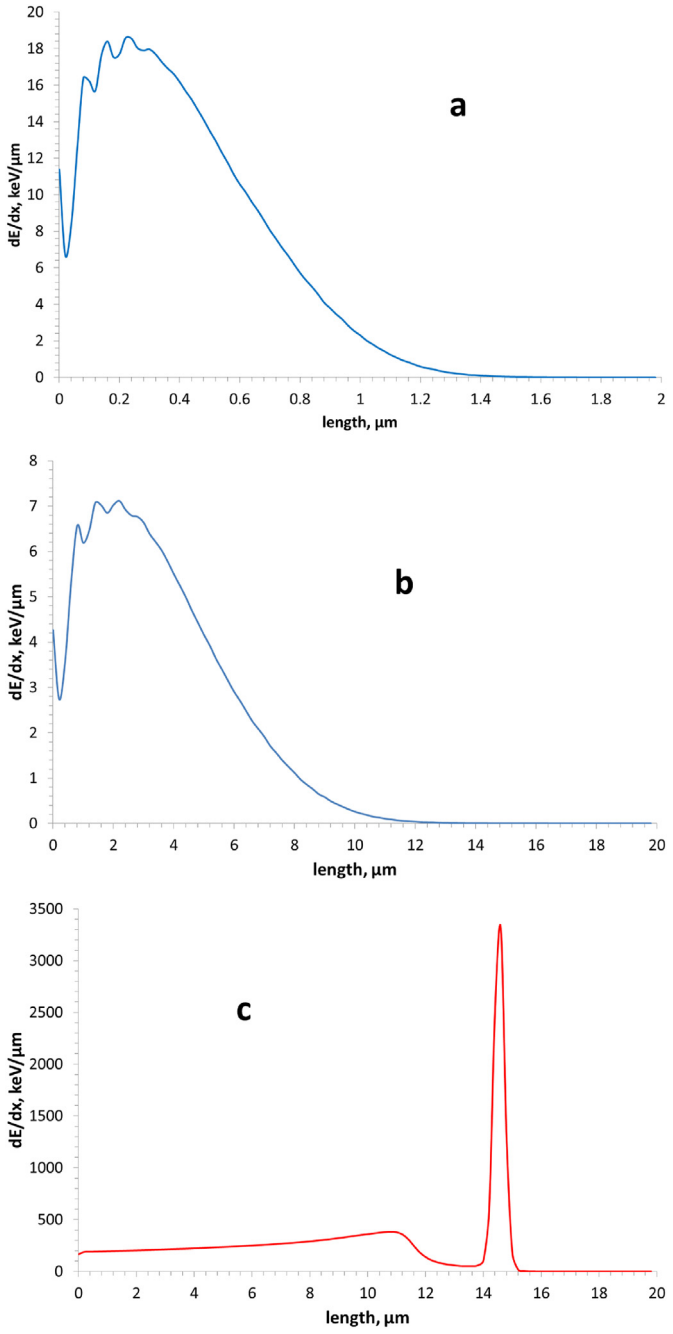

Fig. 6. Energy losses dE/dx of electrons corresponding to an average energy of the emitted β-particles of isotopes ^{63}Ni (a), ^{147}Pm (b) and, α-particles of ^{241}Am (c) in GYAGG matrices with the composition of the sample #3.

There is a room for future improvement of the converters proposed. A gain in LY at excitation with α-particles may be achieved by further optimization of the activator content in the materials. It is well known that γ/α ratio is sensitive to the concentration of the activator and composition of the material at low particles flux excitation [43,44]. At the conditions of a high particle flux excitation, the dominating factor would be the depletion of the activator ground state. Fig. 6 shows comparison of ionization losses *dE* of electrons and α-particles in the Tb doped GYAGG sample.

As seen, for β-particles the 99% of the losses for ionization are in the depth of 1,13 μm for ^{63}Ni, whereas 9,5 μm for ^{147}Pm. The losses for ionization of α-particles are expanded over the 15 μm including the Bragg peak. A maximal number of FTE in the volume created per second is estimated to be: for ^{63}Ni 0.695 mJ/cm^2•0.5/[(3.9•1.6•10^{-19}J) •0.0001 cm] = 5.5•10^{21} cm^{-3}; ^{147}Pm (b) 2.485 mJ/cm^2•0.5/[(3.9•1.6•10^{-19}J) •0.00095 cm] = 2.1•10^{21} cm^{-3}; ^{241}Am: 2.24 mJ/cm^2•0.5/[(3.9•1.6•10^{-19}J) •0.0015 cm] = 1.2•10^{-21} cm^{-3}, whereas an amount of Tb ions is 6.5•10^{20} cm^{-3}. As seen, the concentration of FTE is over the concentration of Tb ions and, in a case of substitution of ^{241}Am by ^{238}Pu will be five times high. Thus, ground state depletion of the Tb^{3+} ions having slowly decaying luminescence kinetics might have an impact on overall converter efficiency towards its decrease. A search of the optimum between gain in the scintillation yield, increase of the doping ions concentration and, a combining in the crystal of a set of doping ions one may get through a future optimization of the indirect converter efficiency.

5. Conclusions

Quaternary Gd–Y compounds with a garnet structure doped with Ce, Tb were found to be a good platform to create high-bright scintillators to be exploited in indirect converters with both β- and α-isotopes. Distinctive features of the developed scintillators are their tolerance to irradiation and temperature stability, what is of especial importance for application in converters. The materials tested were fabricated as ceramics to utilise a flexibility with concentration of doping ions and to achieve high doping levels, which are hardly attained in the single crystalline matrix. All the developed scintillators exhibit the scintillation yield, which is sufficiently high as that of the YAG:Ce material, which is widely used for detectors of ionizing radiation in a wide range of fluxes.

Declaration of competing interest

The authors declare that they have no known competing financial interests or personal relationships that could have appeared to influence the work reported in this paper.

Acknowledgements

Authors with affiliations b, d, e and f acknowledge support from Russian Ministry of Science and Education grant No. 075-15-2021-1353. The scientific equipment provided by shared research facilities “Scientific Research Analytical Center of National Research Center “Kurchatov Institute” – IREA” was used, with financial support of Russian Federation, represented by the Ministry of Science and Higher Education, agreement No. 075-11-2021-070 dated August 19, 2021. The work was partially supported by the Ministry of Science and Higher Education of the Russian Federation (through the basic part of the government mandate, project No. FEUZ-2020-0060) (authors with affiliation “c”).

References

[1] K.E. Bower, Y.A. Barbanel, Y.G. Shreter, G.W. Bohnert, Polymers, Phosphors, and Voltaics for Radioisotope Microbatteries, CRC Press LLC, Boca Raton, 2002.
[2] M.A. Prelas, et al., A review of nuclear batteries, Prog. Nucl. Energy 75 (2014) 117–148.
[3] M.G. Speser, T. Alam, High power direct energy conversion by nuclear batteries, Appl. Phys. Rev. 6 (2019), 0301305.
[4] C. Leroy, P.-G. Rancoita, Principles of Radiation Interaction in Matter and Detection, fourth ed., World Scientific, New Jersey, 2016.
[5] J. Grant, et al., Wide bandgap semiconductor detectors for harsh radiation environments, J.Nucl. Instrum. Methods Phys. Res., Sect. A 546 (2005) 213–217.
[6] J.T. Wacharasindhu, J.W. Kwon, D.E. Meier, J.D. Robertson, Radioisotope microbattery based on liquid semiconductor, Appl. Phys. Lett. 95 (2009), 014103.
[7] S.I. Maximenko, J.E. Moore, C.A. Affouda, P.P. Jenkins, Optimal semiconductors

for 3H and 63Ni betavoltaics, Sci. Rep. 9 (2019) 10892.
[8] M. Eiting, C. J, V. Krishnamoorthy, S. Rodgers, T. George, Demonstration of a radiation resistant, high efficiency SiC betavoltaic, Appl. Phys. Lett. 88 (2006), 064101.
[9] Z. Cheng, X. Chen, H. San, Z. Feng, B. Liu, A high open-circuit voltage gallium nitride betavoltaic microbattery, J. Micromech. Microeng. 22 (2012), 074011.
[10] X.-Y. Li, Y. Ren, X.-J. Chen, D.-Y. Qiao, W.-Z. Yuan, ^{63}Ni Schottky barrier nuclear battery of 4H-SiC, J. Radioanal. Nucl. Chem. 287 (2011) 173–176.
[11] H. Wang, X.-B. Tang, Y.-P. Liu, Z.-H. Xu, M. Liu, D. Chen, Temperature effect on betavoltaic microbatteries based on Si and GaAs under ^{63}Ni and ^{147}Pm irradiation, Nucl. Instrum. Methods Phys. Res., Sect. B 359 (2015) 36–43.
[12] J. Lanley, M. Litz, J. Russo, W. Ray Jr., Design of Alpha-Voltaic Power Source Using Americium-241(^{241}Am) and Diamond with a Power Density of 10mW/cm^3, US Army Research laboratory, October 2017. ARL-TR-8189.
[13] K. Ohno, T. Abe, Bright green phosphor, $Y_3Al_{5-x}Ga_xO_{12}$:Tb, for projection CRT, J. Electrochem. Soc. 134 (1987) 2072.
[14] D.J. Robbins, et al., The relationship between concentration and efficiency in rare-earth activated phosphors, J. Electrochem. Soc. 126 (1979) 1556.
[15] G. Blasse, B.C. Grabmaier, Luminescent Materials, Springer–Verlag, Berlin, 1994.
[16] A. Yamamoto, H, T. Kano, Enhancement of cathodoluminescence efficiency of rare- earth activated Y_2O_2S by Tb^{3+} or Pr^{3+}, J. Electrochem. Soc. 126 (1979) 305.
[17] D.B.M. Klaassen, H. Mulder, C.R. Ronda, Excitation mechanism of cathodoluminescence of oxisulfides, Phys. Rev. B 39 (1989) 42.
[18] Z. Zhang, et al., Application of liquid scintillators as energy conversion materials in nuclear batteries, Sensor. Actuator. A290 (2019) 162–171.
[19] P. Lecoq, A. Gektin, M. Korzhik, Inorganic Scintillators for Detector Systems: Physical Principles and Crystal Engineering, second ed., Springer International Publishing, 2017.
[20] The CERN Large Hadron Collider: Accelerator and Experiments, CERN Document Server, 2009 (accessed June 5, 2021), https://cds.cern.ch/record/1244506.
[21] M. Korjik, E. Auffray, Limits of inorganic scintillating materials to operate in a high dose rate environment at future collider experiments, IEEE Trans. Nucl. Sci. 63 (2016) 552–563.
[22] V. Dormenev, A. Fedorov, M. Glaser, M. Kobayashi, M. Korjik, F. Maas, V. Mechinski, R. Rusack, A. Singovski, R. Zoueyski, Radiation damage of heavy crystalline detector materials by 24 GeV protons, Nucl. Instrum. Methods Phys. Res., Sect. A 701 (2013) 231–234.
[23] E. Auffray, A. Barysevich, A. Fedorov, M. Korjik, M. Koschan, M. Lucchini, V. Mechinski, C.L. Melcher, A. Voitovich, Radiation damage of LSO crystals under γ-and 24GeV protons irradiation, Nucl. Instrum. Methods Phys. Res., Sect. A 721 (2013) 76–82.
[24] E. Auffray, A. Fedorov, M. Korjik, M. Lucchini, V. Mechinski, N. Naumenko, A. Voitovich, Radiation damage of oxy-orthosilicate scintillation crystals under gamma and high energy proton irradiation, IEEE Trans. Nucl. Sci. 61 (2017) 495–500.
[25] R.Y. Zhu, Handbook of Particle Detection and Imaging, Springer, Berlin, 2021, pp. 535–555.
[26] E. Auffray, A. Fedorov, V. Dormenev, J. Houzvicka, M. Korjik, M.T. Lucchini, V. Mechinsky, S. Ochesanu, Optical transmission damage of undoped and Ce doped $Y_3Al_5O_{12}$ scintillation crystals under 24 GeV protons high fluence, Nucl. Instrum. Methods Phys. Res., Sect. A 856 (2017) 7–10.
[27] O. Sidletskiy, I. Gerasymov, D. Kurtsev, et al., Engineering of bulk and fiber-shaped YAGG: Ce scintillator crystals, CrystEngComm 19 (2017) 1001–1007.
[28] V. Alenkov, O. Buzanov, G. Dosovitskiy, et al., Irradiation studies of a multi-doped $Gd_3Al_2Ga_3O_{12}$ scintillator, Nucl. Instrum. Methods Phys. Res., Sect. A 916 (2019) 226–229.
[29] E. Auffray, G. Dosovitskiy, A. Fedorov, I. Guz, M. Korjik, N. Kratochwill, M. Lucchini, S. Nargelas, D. Kozlov, V. Mechinsky, P. Orsich, O. Sidletskiy, G. Tamulaitis, A. Vaitkevičius, Irradiation effects on $Gd_3Al_2Ga_3O_{12}$ scintillators prospective for application in harsh irradiation environments, Radiat. Phys. Chem. 164 (2019) 108365.
[30] C. Dujardin, E. Auffray, E. Bourret-Courchesne, P. Dorenbos, P. Lecoq, M. Nikl, A.N. Vasil'ev, A. Yoshikawa, R.Y. Zhu, Needs, trends, and advances in inorganic scintillators, IEEE Trans. Nucl. Sci. 65 (2018) 1977, 1997.
[31] M. Nikl, A. Yoshikawa, Recent R&D trends in inorganic single-crystal scintillator materials for radiation detection, Adv. Opt. Mater. 3 (2015) 463–481.
[32] N. Cherepy, S.A. Payne, Z. Seeley, P.C. Cohen, M.S. Andreaco, M.J. Schmand, Transparent Ceramic Garnet Scintillator Detector for Positron Emission Tomography, US Pat, 2018, p. 10000698.
[33] G.A. Dosovitskiy, P.V. Karpyuk, P.V. Evpokimov, D.E. Kuznetsova, V.A. Mechinsky, A.E. Borisevich, A.A. Fedorov, V.I. Putlyaev, A.E. Dosovitskiy, M.V. Korjik, First 3d-printed complex inorganic polycrystalline scintillator, CrystEngComm 19 (2017) 4260–4264.
[34] M. Korzhik, V. Alenkov, O. Buzanov, G. Dosovitskiy, A. Fedorov, D. Kozlov, V. Mechinsky, S. Nargelas, G. Tamulaitis, A. Vaitkevičius, Engineering of a new single-crystal multi-ionic fast and high-light-yield scintillation material $(Gd_{0.5}–Y_{0.5})_3Al_2Ga_3O_{12}$:Ce,Mg, CrystEngComm 22 (2020) 2502–2506.
[35] M. Korzhik, A. Borisevich, A. Fedorov, E. Gordienko, P. Karpyuk, V. Dubov, P. Sokolov, A. Mikhlin, G. Dosovitskiy, V. Mechninsky, D. Kozlov, V. Uglov, The scintillation mechanisms in Ce and Tb doped $(Gd_xY_{1-x})Al_2Ga_3O_{12}$ quaternary garnet structure crystalline ceramics, J. Lumin. 234 (2021) 117933.
[36] D.J. Robbins, On predicting the maximum efficiency of phosphor systems excited by ionizing radiation, J. Electrochem. Soc. 127 (1980) 2694–2702.
[37] M.T. Lucchini, V. Babin, P. Bohacek, S. Gundacker, K. Kamada, M. Nikl, A. Petrosyan, A. Yoshikawa, E. Auffray, Effect of Mg^{2+} ions co-doping on timing performance and radiation tolerance of Cerium doped $Gd_3Al_2Ga_3O_{12}$ crystals, Nucl. Instrum. Methods Phys. Res. 816 (2016) 176–183.
[38] A. Potdevin, G. Chadeyron, D. Boyer, R. Mahiou, Optical properties upon vacuum ultraviolet excitation of sol-gel based $Y_3Al_5O_{12}$:Tb^{3+}, Ce^{3+} powders, J. Appl. Phys. 102 (2007), 073536, 073543.
[39] D.M. de Leeuw, G.W. 't Hooft, Method for the analysis of saturation effects of cathodoluminescence in phosphors:applied to Zn2SiO_4:Mg and $Y_3Al_3O_{12}$:Tb, J. Lumin. 28 (1983) 275–300.
[40] E.F. Gibbons, R.G. De Losh, T.Y. Tien, H.L. Stadler, A technique for measuring the saturation of phosphors at high current densities, J. Electrochem. Soc. 120 (1973) 1730–1734.
[41] J.F. Geisz, M.A. Steiner, N. Jain, et al., Building a six-junction inverted metamorphic concentrator solar cell, IEEE J. Photovolt. 8 (2018) 626–632.
[42] E.I. Gorokhova, V.A. Demidenko, S.B. Mikhrin, P.A. Rodnyi, C.W.E. van Eijk, Luminescence and scintillation properties of Gd2O2/S:Tb,Ce ceramics, 2004, IEEE Symp. Conf. Nuc. Sci. 2 (2004) 813–816.
[43] T. Yanagida, H. Takahashi, T. Ito, D. Kasama, T. Enoto, M. Sato, S. Hirakuri, M. Kokubun, K. Makishima, T. Yanagitani, H. Yagi, T. Shigeta, T. Ito, Evaluation of properties of YAG (Ce) ceramic scintillators, IEEE Trans. Nucl. Sci. 52 (2005) 1836–1941.
[44] W.W. Wolszczak, P. Dorenbos, Non-proportional response of scintillators to alpha particle excitation, IEEE Trans. Nucl. Sci. (2017) 1, https://doi.org/10.1109/tns.2017.2699327, 1. doi:.